

# **DEVELOPMENT OF A MICROFLUIDIC MODEL OF A PANCREATIC ACINUS**

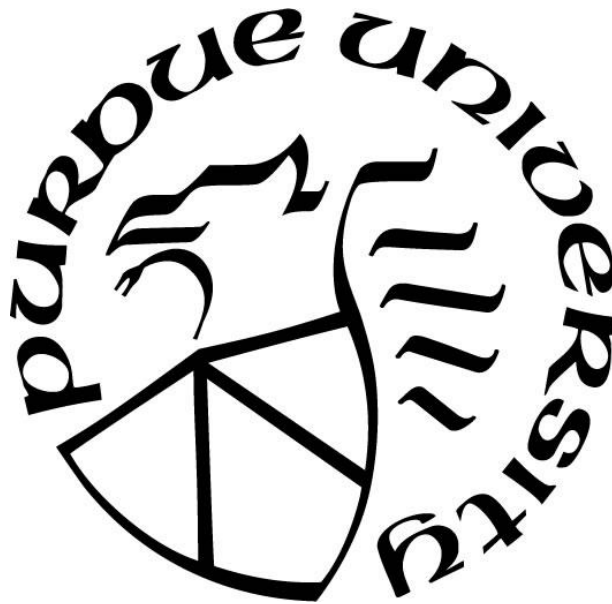
by  
**Stephanie Venis**

**A Thesis**

*Submitted to the Faculty of Purdue University*

*In Partial Fulfillment of the Requirements for the degree of*

**Master of Science in Mechanical Engineering**



School of Mechanical Engineering

West Lafayette, Indiana

August 2019

**THE PURDUE UNIVERSITY GRADUATE SCHOOL**  
**STATEMENT OF COMMITTEE APPROVAL**

Dr. Bumsoo Han, Chair

School of Mechanical Engineering

Dr. Stephen F. Konieczny

Department of Biological Sciences

Dr. Amy M. Marconnet

School of Mechanical Engineering

**Approved by:**

Dr. Jay Gore

Head of the Graduate Program

*This work is dedicated to my boyfriend, parents, grandparents, and brother.*

## **ACKNOWLEDGMENTS**

I would like to acknowledge my advisor, Dr. Bumsoo Han, as well as my committee members Dr. Stephen F. Konieczny and Dr. Amy Marconnet, for their support and critiques which were instrumental to the success of this work. I would like to thank Dr. Yi Yang, Hye-ran Moon, and all members of the Biotransport Phenomena Laboratory for their help and input on this work. Finally, I would like to acknowledge the Purdue Imaging Facility for their help in the collection of the visible confocal and second harmonic generation images included herein.

## TABLE OF CONTENTS

LIST OF FIGURES .....	6
ABSTRACT.....	8
1. INTRODUCTION .....	10
2. METHODS .....	13
2.1 Device Fabrication .....	13
2.2 Acquisition of Cell Line.....	13
2.3 Cell Culture .....	14
2.3.1 Normal Culture .....	14
2.3.2 Induction Culture .....	14
2.4 Creation of Acinus and Cell Seeding.....	14
2.5 Microscopic Characterization .....	19
2.6 RT-qPCR.....	19
2.7 Statistical Analysis.....	19
3. RESULTS .....	20
3.1 Culture of Panc1-Tet-PTF1a in AMOC.....	20
3.2 Confirming Acinar Characteristics .....	22
3.3 Confirmation of Induction .....	25
4. DISCUSSION.....	26
5. CONCLUSION.....	28
REFERENCES .....	30
APPENDIX.....	34

## LIST OF FIGURES

Figure 2-1: Healthy pancreatic acini. (A) Many acini within healthy human pancreatic tissue, with two individual acini circled. Scale bar represents 50 $\mu\text{m}$ . (B) Simplified schematic of a single acinus. Large acinar cells containing zymogen granules and ductal cells leading away from acinus. ....	15
Figure 2-2: (A) A schematic of the acinar tumor microenvironment on a chip showing collagen and cells and (B) the schematic with a section cut away to expose the inner cavity of the device. ....	16
Figure 2-3: Schematic outlining the key steps in loading the AMOC. ....	17
Figure 2-4: Formation of the duct and acinus within the collagen matrix as indicated by the dark dyed culture medium progressing through the chip. Scale bar represents 300 $\mu\text{m}$ . ..	18
Figure 3-1: Acinar end of chip with or without Dox after 1, 3, 5, 7, 9, and 11 days of culture. The white box on the day 1 images indicates the enlarged region in the lower row of each culture condition (-Dox or + Dox). Scale bars represent 250 $\mu\text{m}$ . ....	21
Figure 3-2: (A) 3D reconstruction of bottom half of acinus from control case. Arrow indicates sprouts into the collagen matrix. (B) 3D reconstruction of treated case showing no sprouts. Scale bar represents 500 $\mu\text{m}$ . ....	22
Figure 3-3: SHG images showing type I collagen matrix (naturally fluorescing) and cell nuclei (DAPI). Single focal plane showing the thickness of the lumen in the (A) untreated and (B) treated samples. 3D reconstruction of (C) the untreated sample showing the collagen matrix near invading cells, indicated by arrows, and (D) the treated sample showing alignment of collagen fibers along lumen wall, indicated by arrows. Scale bar represents 50 $\mu\text{m}$ . ....	24
Figure 3-4: Relative transcript levels of PTF1a and the downstream target gene, PRSS2, after 3 days of culture in the chip. * $p < 0.05$ , ** $p < 0.01$ , *** $p < 0.001$ . ....	25
Figure A-1: Molds for the (A) top and (B) bottom of the chip .....	34
Figure A-2: Side view of assembled chip showing relevant dimensions. ....	34
Figure A-3: Chip assembly process .....	35
Figure A-4: Panc1 culture with and without Dox. White box in day 1 images show the enlarged region in subsequent days. Scale bars represent 250 $\mu\text{m}$ . ....	36

Figure A-5: RT-qPCR results. Relative transcript levels of (A) PTF1a and (B) PRSS2 for 3D culture of the untreated case (-Dox), the case in which the cells first received Dox in 2D (+Dox 2D induction) and the case in which the cells first received Dox treatment once in the chip (+Dox 3D induction) ..... 37

Figure A-6: Morphological comparison of the cells induced 2D and 3D then grown in 3D culture for the first 5 days of culture..... 38

## ABSTRACT

Author: Venis, Stephanie, M. MSME  
Institution: Purdue University  
Degree Received: August 2019  
Title: Development of a Microfluidic Model of a Pancreatic Acinus  
Committee Chair: Dr. Bumsoo Han

Pancreatic Ductal Adenocarcinoma (PDAC) continues to have a dismally low survival rate due to late diagnosis and poor treatment options. Therefore, there is a need to understand the early stages and progression of the disease. PDAC is known to have two types of cells of origin: ductal cells or acinar cells. Since acinar-derived PDAC is thought to be the more malignant of the two, it was chosen as the focus of this work. Most studies of acinar cells as they relate to PDAC are accomplished by using animal models such as genetically engineered mouse models. While this method yields a large amount of insight into the progression of the disease and the role of specific genes, it has the drawbacks of being very time and resource intensive. The quicker and less costly alternative is *in vitro* culture. Specifically, here we have developed a microfluidic model which can incorporate a key aspect of the extracellular matrix (ECM), type I collagen, and mimics the 3D geometry of an *in vivo* acinus. Most attempts at *in vitro* culture have been limited by the fact that isolated acinar cells show a decrease in the amount of digestive enzymes they secrete as culture continues. For this reason, we are using a reprogrammed cancer cell line. These cells can be induced with doxycycline to express PTF1a, which allows the cells to adapt acinar characteristics, such as the production of digestive enzymes. We were able to successfully culture and induce PTF1a in these cells within our chip. We showed that the cells exhibit no invasion into the collagen matrix once PTF1a is expressed, thus eliminating a key aspect of cancer cell culture. The cells grown in the chip are confirmed to be producing PRSS2, the digestive enzyme trypsinogen. Collectively, this suggests that we have produced healthy



acinar cells growing in the same configuration that they would *in vivo*. This has many applications in the study of pancreatic ductal adenocarcinoma, as we have developed way to culture reprogramed cancer cells as their benign precursors and maintain acinar characteristics *in vitro*. It will also have applications in the study of many other pancreatic diseases by providing an *in vitro* model of a healthy, functional acinus.

## 1. INTRODUCTION

Pancreatic ductal adenocarcinoma (PDAC) remains one of the deadliest ailments with an average 5-year survival rate of 9% [1]. This poor prognosis is largely attributed to the late detection of the disease and minimal successful treatment options. Therefore, there is a great need to understand the early stages and development of the disease in order to diagnosis it sooner and treat it more effectively. It was originally believed that this disease arose from mutated ductal cells [2], [3], but other studies have indicated that acinar cells may be the progenitors of PDAC [4]–[7]. Recently, one study explored both groups as potential precursors of the disease and showed the morphological differences in the resulting PDAC. They showed that PDAC from acinar origins gave rise pancreatic interepithelial neoplasia (PanINs) as a key step in the progression to PDAC; whereas, ductal-derived PDAC did not form PanINs as an intermediate [8]. When considering both ductal and acinar cells as potential sites of origin, acinar-derived PDAC seems to be more malignant and may be associated with a worse prognosis [9], [10]. Therefore, the focus of the current work is PDAC of acinar origin.

Acinar cells are secretory cells within the pancreas that are responsible for the production, packaging, and secretion of digestive enzymes. These large cells form circular acini that branch from the ducts which carry away the digestive enzymes. When acinar cells start exhibiting markers of ductal cells, they are said to have undergone acinar to ductal metaplasia (ADM). Acinar cells lose the ability to produce and secrete digestive enzymes, lose their polarity, and begin to exhibit ductal cell morphology and proteins. ADM can occur as a result of pancreatitis or injury, though without oncogenic KRAS mutations the process is reversible [11]–[13]. However, in the presence of oncogenic KRAS this change becomes permanent and PanIN lesions and PDAC can develop [5], [14]–[17]. Acinar cells have proven very difficult to culture

*in vitro* as they tend to lose many of their identifying characteristics such as polarity and secretory capabilities within hours [18] or days [19], [20] of isolation. Therefore, many *in vitro* studies of these cells are limited in that they must be completed soon after isolation of the cells [21], [22]. For this reason, we will be using reprogrammed cancer cells. These cells are much more robust in *in vitro* culture, immortalized, and can be selectively induced to express the gene of interest, PTF1a. PTF1a is responsible for the production of digestive enzymes, and is known to be absent or decreased in PDAC [23], [24]. When PTF1a is silenced, acinar cells progress much more quickly through ADM and develop into PDAC [23].

There are currently a variety of models to study the role acinar cells in PDAC *in vivo* and a few *in vitro*, each with their own advantages and disadvantages. Genetically engineered mouse models (GEMMs) allow for the study of specific gene mutations within a living system that closely resembles the physiology and architecture of the human pancreas, making them the ideal option for pre-clinical drug trials and study of specific genes. Many groups have shown that inducing mutations in KRAS and the tumor suppressor gene p53 within adult acinar cells in mice will give rise to PanIN lesions and result in PDAC [8], [9], [24]. GEMMs have given many insights into the disease but are limited by the ethical concerns, high cost, and time demands associated with this method [25]. Additionally, the model is very complex; it can be difficult to isolate the effects of a specific gene on the progression of the disease due to the combinations of other cell types and growth factors found in the microenvironment. To combat this, many groups have successfully isolated cells from specific GEMMs and from actual human tumors for *in vitro* study. Culture methods have been optimized for these cells to allow for inexpensive and simple growth of the cells [25], [26]. This provides a great deal of information about the specific cell type and allows for preliminary drug testing before moving to GEMMs. However, growing cells

in 2D lacks relevance to the natural cellular microenvironment in terms of mechanical and chemical signals which are neglected. This has been shown in many cases to affect the behavior of the cells [26]–[28].

In recent years, *in vitro* studies are moving towards 3D models which can better replicate the cellular microenvironment. These cultures can come in a variety of forms: single cells or cell spheroids suspended in ECM-like components, cells grown on scaffolds, microfluidic chips, etc. [25], [29]–[32]. Cells cultured in any of these platforms are more closely related to *in vivo* characteristics. Aspects of the tumor microenvironment (TME) which are entirely neglected in simple 2D models, can be added into the model by way of adding ECM components, which help in mimicking the natural mechanical forces exerted on and by the cells, or by selectively adding different cell types, which allows for cell-cell signaling [27], [33]–[37]. Microfluidic devices offer endless possibilities in geometrical configurations. They can mimic *in vivo* structures, create compartments for additional cell types, or channels for the introduction of chemical factors. Microfluidic chips offer a suitable compromise between GEMMs and 2D culture, with their main limitation being that it takes a certain level of training and specialized equipment to be able to use them [25].

The current work aims to create a microfluidic chip which will mimic the *in vivo* geometry of a pancreatic acinus to culture PDAC cells which can be manipulated to become acinar cells. Reprogramming cancerous cells to become their healthy precursor would provide a novel way of treating PDAC which has proven resistant to many other treatments. Panc1-Tet-PTF1a cells lose their malignant properties and begin producing digestive enzymes after PTF1a induction [24]. The current microfluidic platform adds two key components of acini found in pancreata *in vivo*: a type I collagen ECM and a similar 3D geometry.

## **2. METHODS**

### **2.1 Device Fabrication**

Devices were fabricated from a polydimethylsiloxane (PDMS, Dow Corning, Midland, MI) solution, comprised of base and curing agent, on a 3D printed mold, shown in the appendix Figure A-1. The solution was set to cure at 80°C for four hours then removed from the mold to yield materials for 28 chips. Inlet and outlet holes were created in the top half of the chip using a 2 mm biopsy punch through the guide impressions from the mold. Using a 3 mm biopsy punch, a hole was cut into the bottom half of the mold through the guide impression. This hole will align with the 3 mm cylindrical cavity in the top half of the chip to create a chamber for the acinus to form, such that the matrix will be in direct contact with the glass slide. Each half of the chip was thoroughly cleaned of dust and debris, then treated with a corona discharger (Electro Technic Product, Inc., Chicago, IL) and affixed together. The assembled device was treated again with the corona discharger and adhered to a glass microscope slide. A schematic of the fabrication process can be seen in the appendix Figure A-3.

### **2.2 Acquisition of Cell Line**

Panc1-Tet-PTF1a are human-derived PDAC cells, which have been genetically modified to allow for the pancreatic transcription factor 1a (PTF1a) gene to be expressed in the presence of doxycycline. This cell line was engineered in Dr. Stephen F. Konieczny's lab at Purdue University. Further details about the acquisition and modification of this cell line is described by Jakubison et al. [24].

## **2.3 Cell Culture**

### **2.3.1 Normal Culture**

Cells were cultured in tissue culture treated flasks (Fisher Scientific, Hampton, NH) with Dulbecco's Modified Eagle's Medium (Sigma-Aldrich, Darmstadt, Germany) supplemented with 10% Tet system approved fetal bovine serum (Takara Bio USA, Inc., Mountain View, CA), GlutaMAX™ supplement (Gibco, Carlsbad, CA), and 10,000 U/mL penicillin-streptomycin (Gibco, Carlsbad, CA). Cells were cultured until reaching approximately 80% confluency, then harvested for sub-passaging or experimentation.

### **2.3.2 Induction Culture**

In the case of induced Panc1-Tet-PTF1a, cells were cultured in Dulbecco's Modified Eagle's Medium (Sigma-Aldrich, Darmstadt, Germany) supplemented with 10% Tet system approved fetal bovine serum (Takara Bio USA, Inc., Mountain View, CA), GlutaMAX™ supplement (Gibco, Carlsbad, CA), 10,000 U/mL Penicillin-Streptomycin (Gibco, Carlsbad, CA), and 1 µg/mL doxycycline hyclate (Cat. D3447, Sigma, St. Louis, MO, USA) after being seeded in the chip.

## **2.4 Creation of Acinus and Cell Seeding**

Within the chip described above, a duct leading into an acinus can be created within a collagen matrix and lined with cells. The geometry mimics that of an *in vivo* acinus depicted below in Figure 2-1.

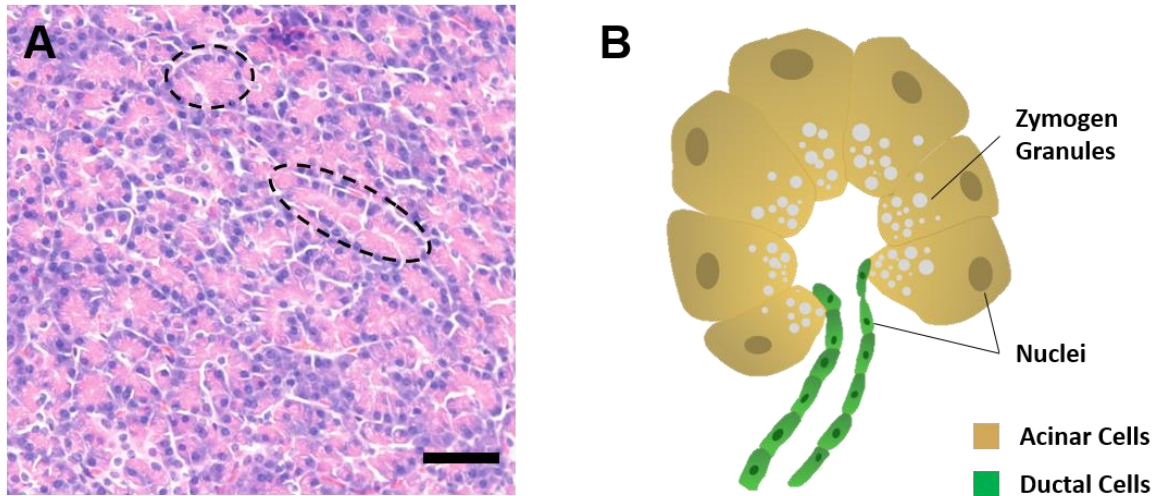


Figure 2-1: Healthy pancreatic acini. (A) Many acini within healthy human pancreatic tissue, with two individual acini circled. Scale bar represents 50  $\mu\text{m}$ . (B) Simplified schematic of a single acinus. Large acinar cells containing zymogen granules and ductal cells leading away from acinus.

The resulting configuration of cells and matrix within our chip is shown in Figure 2-2. The cells are surrounded in a type I collagen matrix which is a primary component of the native extra cellular matrix [38]. Therefore, the resulting microfluidic device has been named acinar microenvironment on a chip (AMOC). The dimensions of the chip are provided in the appendix Figure A-2.

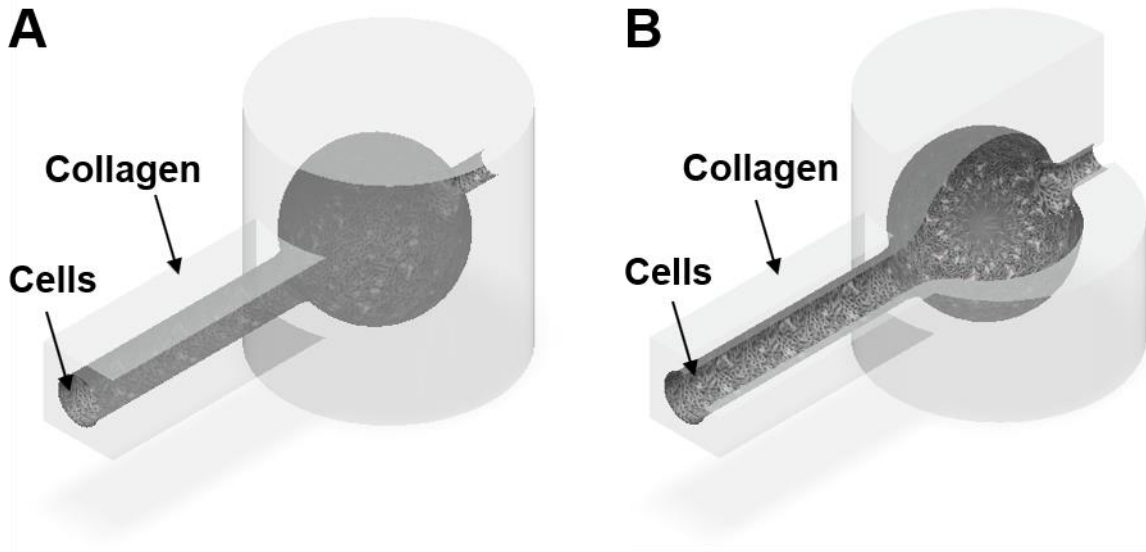


Figure 2-2: (A) A schematic of the acinar tumor microenvironment on a chip showing collagen and cells and (B) the schematic with a section cut away to expose the inner cavity of the device.

The chip is first filled with a type I collagen solution derived from rat tail (Corning, Corning, NY). Then a 7  $\mu$ L droplet of culture medium is placed on the inlet port. Collagen solution is removed from the outlet to pull the medium into the chip and form a duct ending in an acinus via viscous fingering [39]. The chip is incubated at 37 °C for 15 minutes to allow the collagen to polymerize. The acinus is then pierced with a 34G needle to allow medium to flow through the chip from inlet to outlet. This outlet channel is kept as small as possible so as to minimally deviate from the normal acinar architecture. Finally, cells are loaded into the chip. This process is depicted in Figure 2-3.



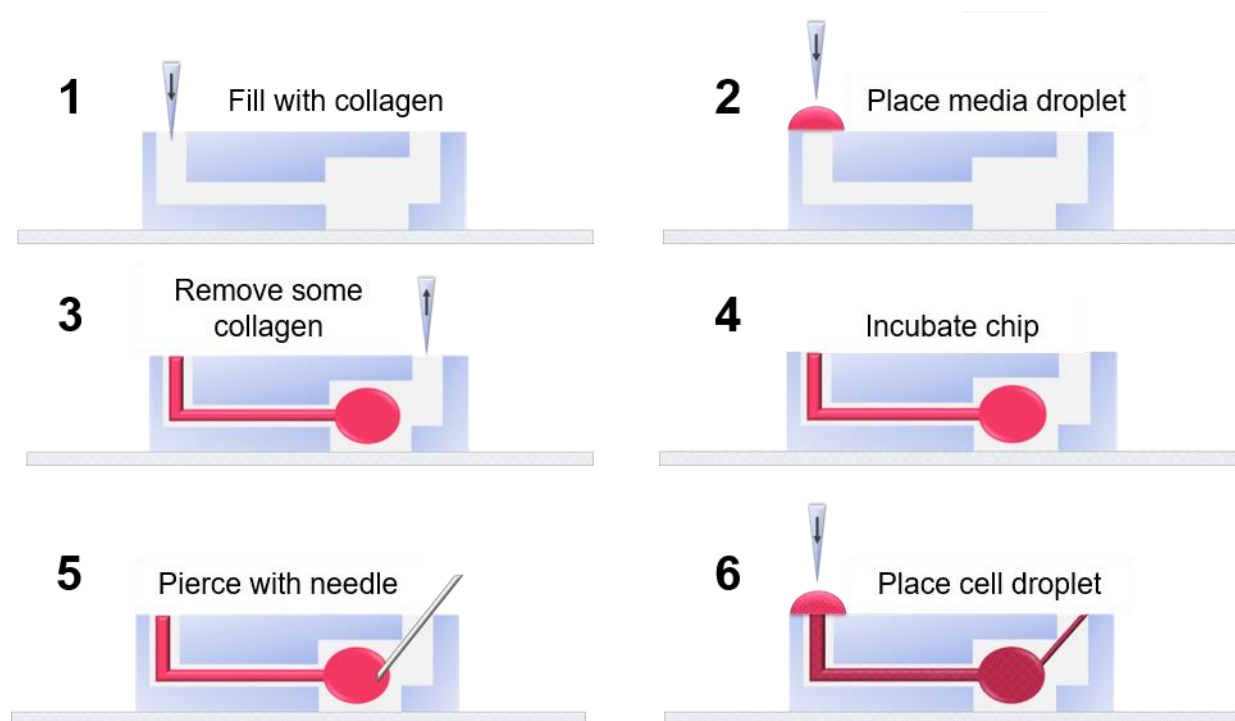


Figure 2-3: Schematic outlining the key steps in loading the AMOC.

Step 3 as illustrated in Figure 2-3 requires that a small amount of collagen solution is removed from the outlet which pulls the media from the droplet resting on the inlet port. When this is done, the duct and acinus are formed within the collagen as the geometry of the chip changes. Figure 2-4 shows sequential frames of this process with dyed media being used for visualization purposes.

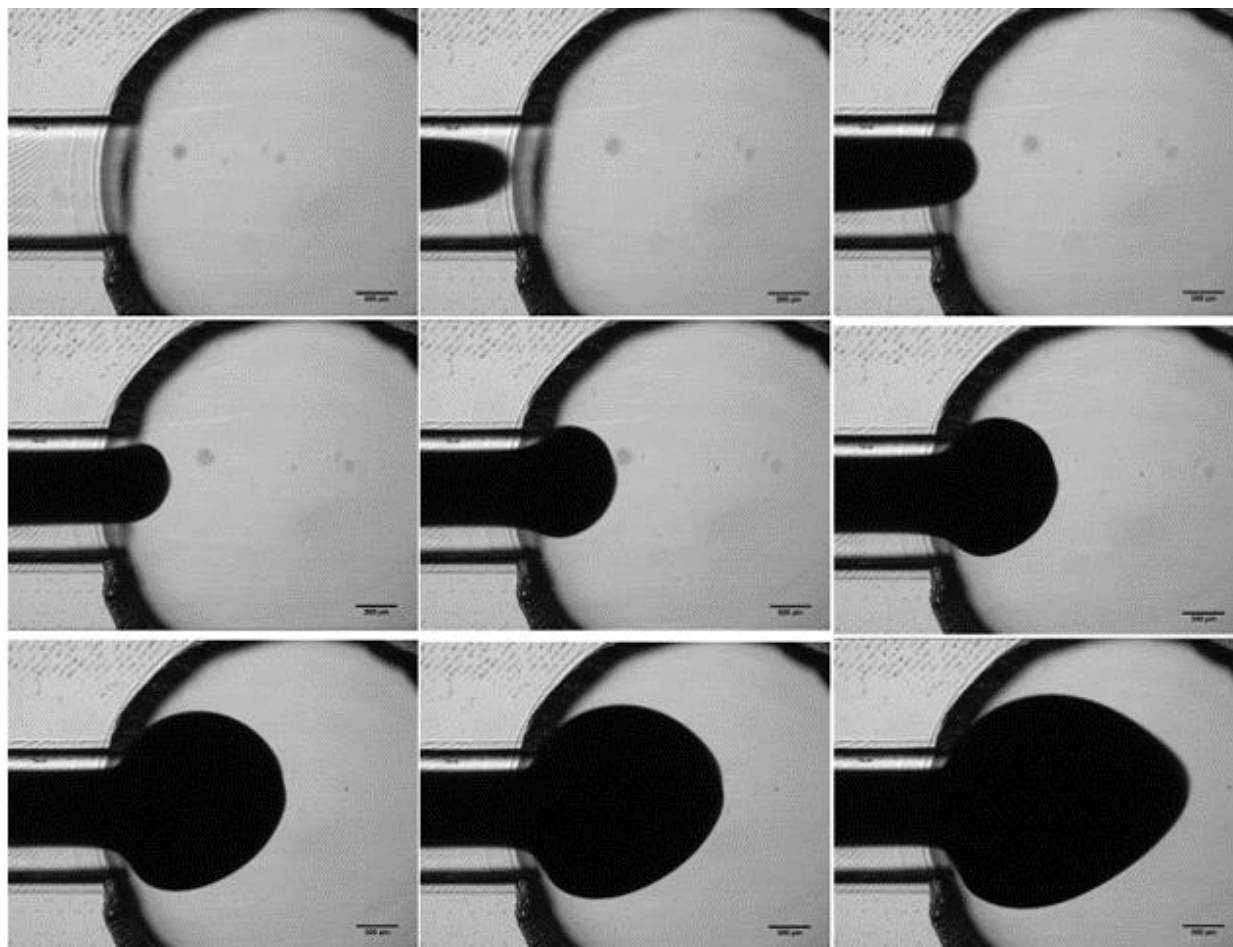


Figure 2-4: Formation of the duct and acinus within the collagen matrix as indicated by the dark dyed culture medium progressing through the chip. Scale bar represents 300  $\mu\text{m}$ .

The final step specified in Figure 2-3 is cell loading. A 10  $\mu\text{L}$  droplet of cell suspension (5,000 cells/ $\mu\text{L}$  of culture medium) is placed on the inlet and allowed to fill the chamber. The chip is incubated at 37  $^{\circ}\text{C}$  for 15 minutes to allow the cells to adhere to the collagen along the bottom of the chip. Then fluid is removed from the outlet and another 10  $\mu\text{L}$  droplet of cell suspension can be added. The chip is rotated 90 $^{\circ}$  and incubated again to allow cells to adhere to the side wall of the chip. This step is repeated two more times so that all sides of the chamber are covered in a uniform cell layer. Finally, reservoirs were added to the inlet and outlet to allow for perfusion of culture medium, and the inlet reservoir was filled.

## 2.5 Microscopic Characterization

For confocal imaging, the samples were incubated for 30 minutes with culture medium containing a 1:1000 dilution of CellMask Deep Red (Invitrogen, Carlsbad, CA) and 10  $\mu\text{g/mL}$  of Hoechst 33342 (Sigma-Aldrich, St. Louis, MO) to stain the cell membranes and nuclei, respectively. The samples were then fixed in 4% formaldehyde solution for 10 minutes and rinsed thrice with DPBS (Gibco, Carlsbad, CA). The samples were then imaged with a Nikon Multiphoton Intravital system. We used both visible confocal and multiphoton second harmonic generation methods for imaging.

## 2.6 RT-qPCR

Gene expression of Panc1-Tet-PTF1a with and without doxycycline treatment was characterized by RT-qPCR after seeding to confirm the successful induction of PTF1a. Cells were harvested from the devices and RNA was collected using a miRNeasy Mini kit (Qiagen, Cat.217004, Hilden, Germany). Total RNA could then be changed into cDNA using the iScript cDNA synthesis kit (Bio-Rad, Cat 1708891, Hercules, CA). RT-qPCR was then completed using SYBR green (Roche, cat. 04913850001, Indianapolis, IN). PTF1a and PRSS2 genes analyzed here were normalized using 18S as an internal control. The standard  $\Delta\Delta\text{Ct}$  method was used to determine the changes in levels of each gene.

## 2.7 Statistical Analysis

For the comparison of results in the RT-qPCR experiments, groups were compared using a one-tailed t-test, with each group containing two-three biological replicates. Statistical significance is denoted in terms of p-values, where  $p < 0.05$  was considered statistically significant. Error bars denote mean  $\pm$  standard deviation. \* $p < 0.05$ , \*\* $p < 0.01$ , \*\*\* $p < 0.001$ .

### 3. RESULTS

#### 3.1 Culture of Panc1-Tet-PTF1a in AMOC

Panc1-Tet-PTF1a cells were loaded into the chips following the protocol outlined above in Figure 2-3. Half of the chips were treated with culture medium containing doxycycline on day 0 after loading and the other half served as the control with normal culture medium. The media was replaced daily with normal or Dox-containing media. The chips were cultured for 14 days and daily images were captured to observe any morphological differences in the two groups. Representative images from this culture are shown in Figure 3-1. When PTF1a is expressed, the cells have been shown to exhibit acinar characteristics [24]. Acinar cells are not actively proliferating and are not invasive into the surrounding matrix as cancer cells are. These changes are observed below in that the -Dox case shows many cellular protrusions into the collagen whereas the cells treated with Dox show very little invasion into the matrix even after nearly 2 weeks of culture.

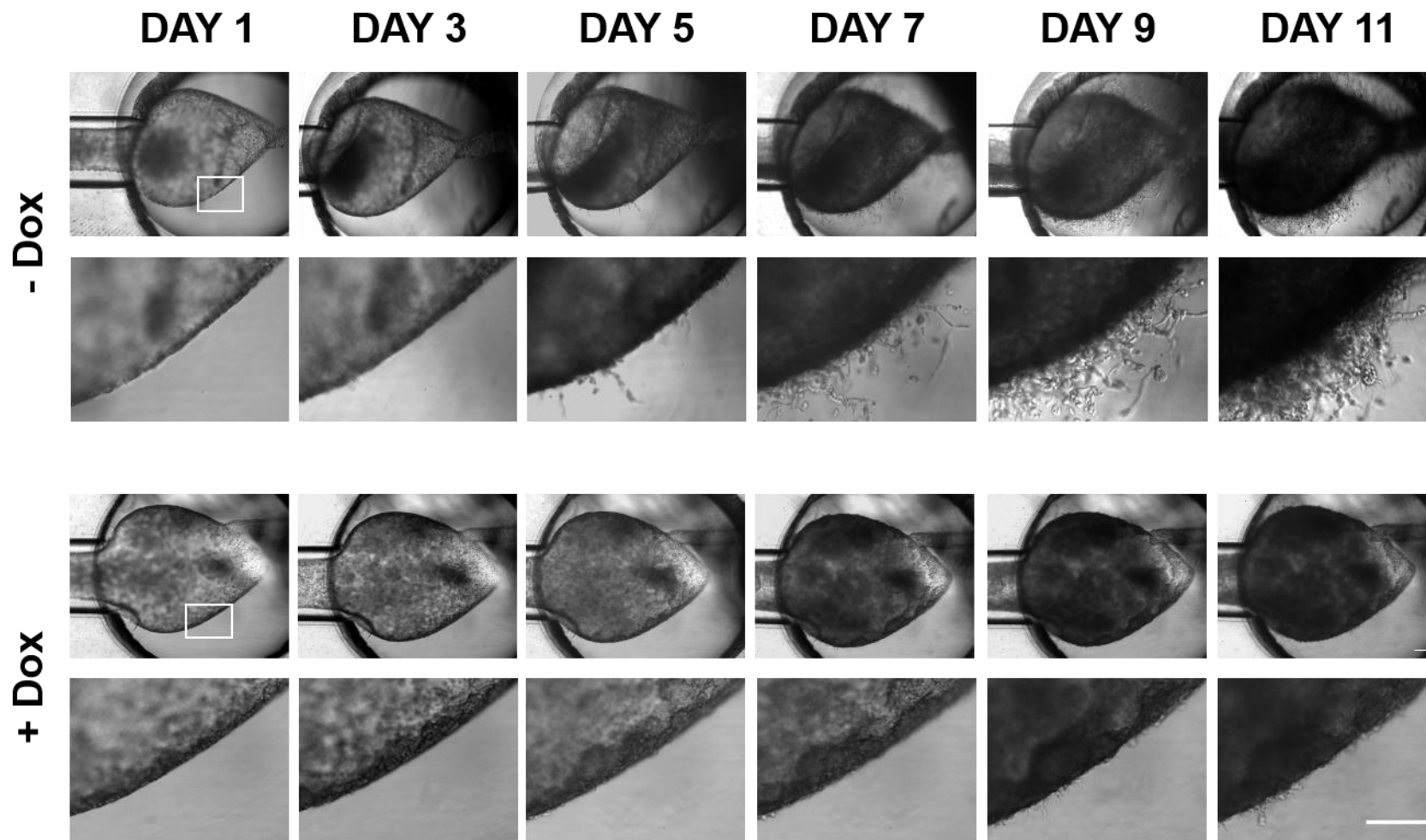


Figure 3-1: Acinar end of chip with or without Dox after 1, 3, 5, 7, 9, and 11 days of culture. The white box on the day 1 images indicates the enlarged region in the lower row of each culture condition (-Dox or + Dox). Scale bars represent 250  $\mu\text{m}$ .

### 3.2 Confirming Acinar Characteristics

With the use of confocal imaging, we are able to confirm the geometry of the acinus. Only the bottom half of the device was imaged. The result is a hollow sphere lined with cells as shown in Figure 3-2. After Dox treatment, it has been shown [24] that the cells are no longer actively proliferating. Additionally, since they are now more like acinar cells than cancer cells, their invasion patterns are altered. It can be seen that there are no sprouts into the collagen in the treated case.

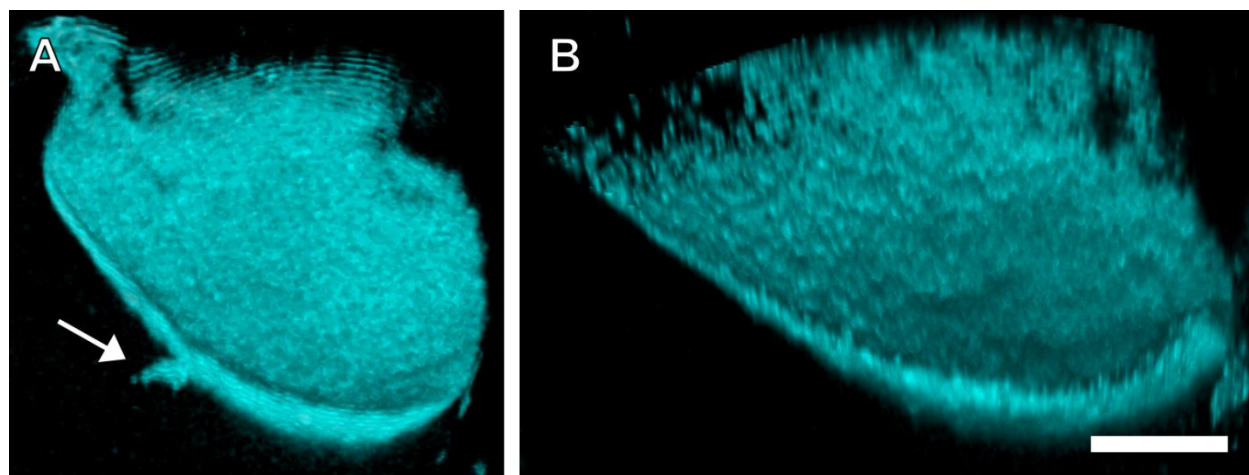


Figure 3-2: (A) 3D reconstruction of bottom half of acinus from control case. Arrow indicates sprouts into the collagen matrix. (B) 3D reconstruction of treated case showing no sprouts. Scale bar represents 500  $\mu\text{m}$ .

Second harmonic generation (SHG) was used to identify the collagen fibers without staining. Due to the fact type I collagen is nonsymmetric and highly crystalline, it produces a very clear second harmonic signal [40]. The nuclei were stained to indicate the locations of the cells and fluoresce on a similar wavelength to the collagen. When looking at a single focal plane within the SHG images, it can first be seen that the thickness of the cell layer is very different between the untreated and treated cases Figure 3-3 (A-B). After induction of PTF1a, the cells are

no longer actively proliferating, unlike the cancer cells in the -Dox case. Therefore, we would expect to see a much greater cell number in the untreated than the treated case. The -Dox case shows a multicell layer, while the treated case shows a monolayer which indicates that these cells are now more like acinar cells than cancer cells in their growth patterns.

When comparing how cells interact with the surrounding collagen matrix, it is necessary to consider the invasions. In the absence of sprouts, the cells have a much different impact on the collagen around them. As can be seen in the untreated sample, Figure 3-3 (C), the collagen matrix near the emerging invasion is much less dense, and the fibers are aligned along the outside of the cells in the longer invasion, perpendicular to the acinus. The cells are pulling on the collagen fibers and forcing alignment to allow for the movement of the cells away from the epithelial sheet and through the matrix. Alternatively, the treated cells show no invasion points and so a different relationship with the collagen. In the case of +Dox cells, the collagen matrix shows a decrease in density near the cell layer and alignment of collagen fibers along the outside wall, as shown below in Figure 3-3 (D).



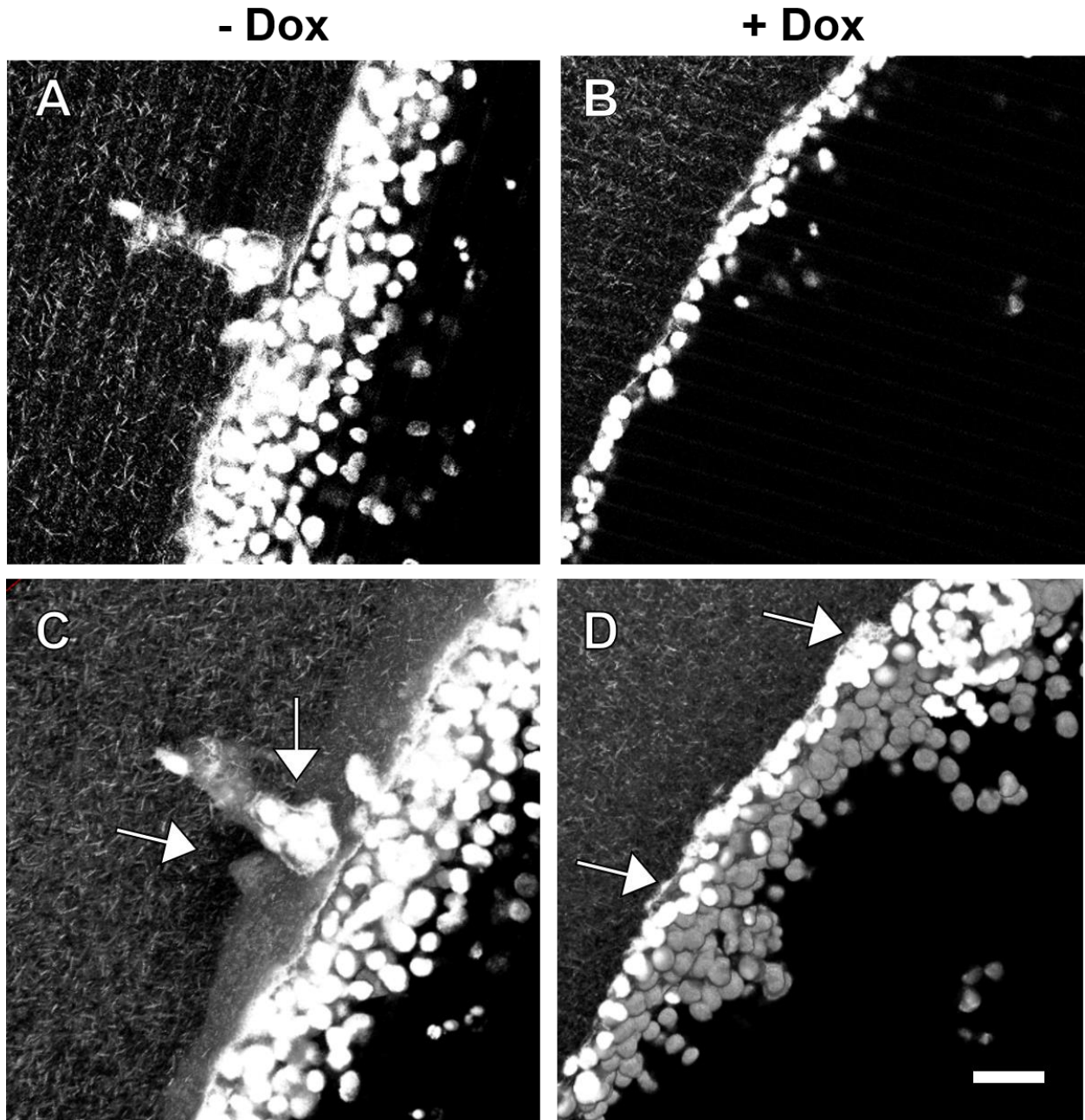


Figure 3-3: SHG images showing type I collagen matrix (naturally fluorescing) and cell nuclei (DAPI). Single focal plane showing the thickness of the lumen in the (A) untreated and (B) treated samples. 3D reconstruction of (C) the untreated sample showing the collagen matrix near invading cells, indicated by arrows, and (D) the treated sample showing alignment of collagen fibers along lumen wall, indicated by arrows. Scale bar represents 50  $\mu\text{m}$ .



### 3.3 Confirmation of Induction

Panc1-Tet-PTF1a was developed so that the PTF1a gene would be expressed in the presence of doxycycline [24]. It was necessary to confirm that the genes could be induced in the same way as shown previously [24] in 2D and when cultured in our microfluidic platform. RT-qPCR was performed to quantify the relative mRNA transcripts for PTF1a, the gene of interest, and PRSS2, a downstream target gene which encodes for the digestive enzyme trypsinogen. As shown in Figure 3-4, it can be seen that expression of both genes was significantly increased when treated with Dox as compared to the -Dox case in both 2D and 3D culture conditions.

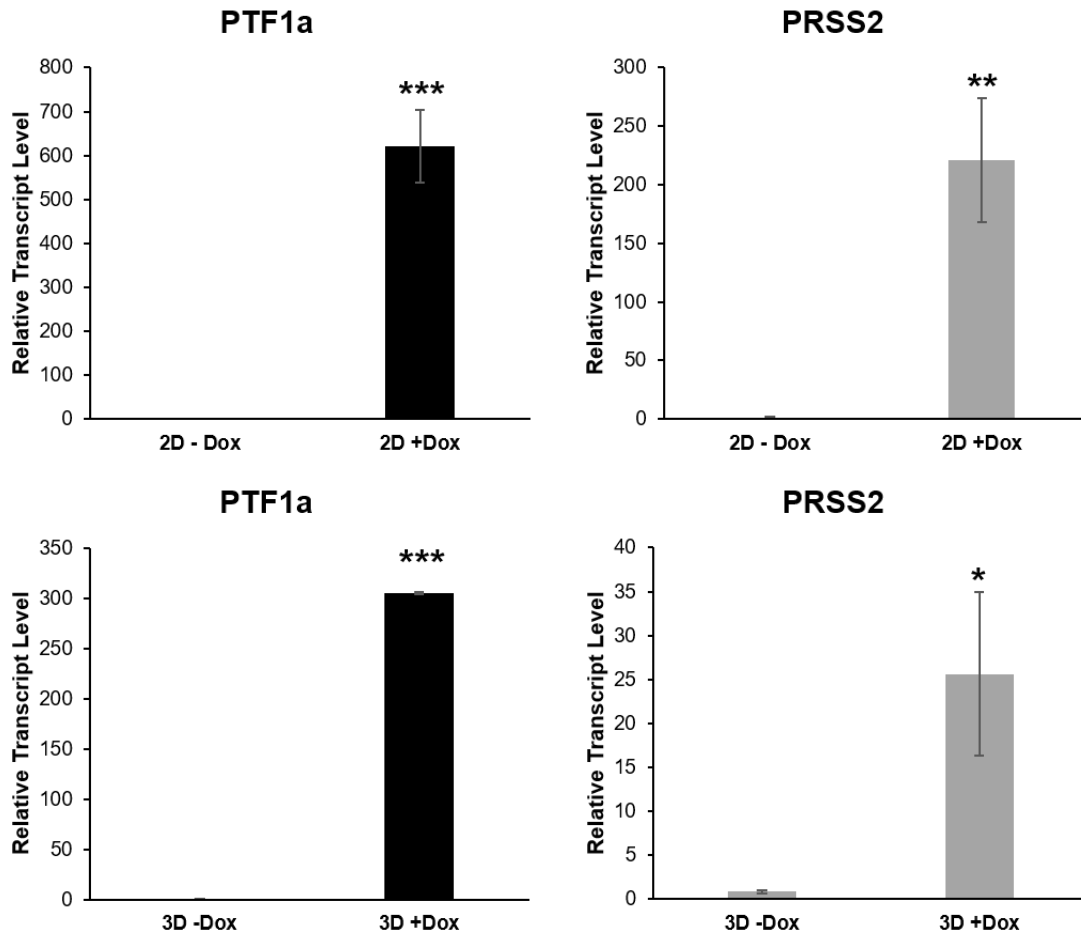


Figure 3-4: Relative transcript levels of PTF1a and the downstream target gene, PRSS2, after 3 days of culture in the chip. \* $p < 0.05$ , \*\* $p < 0.01$ , \*\*\* $p < 0.001$ .

## 4. DISCUSSION

The developed microfluidic device, acinar microenvironment on a chip, gives an *in vitro* method to study pancreatic acini as they relate to pancreatic ductal adenocarcinoma. This chip provides an advantage over current methods, because the cells are constrained into a physiologically relevant geometry which adds an additional level accuracy to the *in vitro* culture. In this way, we are able to assess the change in invasion patterns due to the expression of PTF1a. Panc1 cells are known to be highly invasive into the collagen matrix (appendix Figure A-4), but after Dox treatment, the cells exhibit little to no invasion into the matrix. This further supports that expression of PTF1a reduces the malignancy of the cancer cells. Similarly, it has been shown that adult acinar cells are not actively proliferating [41], so we expect to see a thinner lining of the lumen in the treated case. This was confirmed when looking at a single focal plane from the confocal images. While the samples largely show the acinar characteristics that we expect to see, there are a few regions in the treated samples that are thicker or might show small sprouts into the collagen. Only about 85% of the treated cells will express PTF1a [24] after Dox treatment, therefore it is expected that the part of the population which is unchanged will exhibit the same characteristics as the untreated case.

Using SHG imaging, we were also able to gain some insight into the interaction between the cells and the surrounding collagen matrix. In the untreated case, the invading cells are remodeling the collagen matrix to allow for easier movement away from the lumen. This is similar to the collagen alignment around PDAC tissue *in vivo*. Alternatively, a thin layer of type I collagen is found concentrically around acinar lobules *in vivo* [38], which is very similar to the collagen alignment shown above in Figure 3-3.

In order to show the relevance of this model in producing a functional acinus, we need to confirm that the cells are producing digestive enzymes. We were able to successfully show that transcripts for PTF1a and the downstream gene for trypsinogen, PRSS2, are expressed in the presence of doxycycline in 3D culture in the same way that it is in 2D. Thus, our *in vitro* platform yields a model of a functional pancreatic acinus in respect to geometry and digestive enzyme production.

## 5. CONCLUSION

The acinar microenvironment on a chip platform provides a reliable *in vitro* method of mimicking a pancreatic acinus to study the role of acinar cells in PDAC, both in the development and the potential treatment of the disease. Due to the current inability to successfully culture acinar cells *in vitro* for extended periods of time, this method of using reprogrammed cells opens a wide range of possibilities for the study of this cell type. In this study, the treated cells yielded an *in vitro* model of a healthy acinus with functional acinar cells. This has applications not only in the study of PDAC, but also in studying the role of acini in other pancreatic diseases such as type I diabetes [42], chronic pancreatitis [43], or alcoholic pancreatitis [44].

Alternatively, we have also shown in the untreated case, that cancerous epithelial cells can be grown in this model. In duct-derived PDAC, it was shown that tufting and loss of polarity occurs in the earlier stages of disease progression [8]. When used to culture cancer cells, the variation in geometry from the duct to the acinus within the developed chip can also be used to study these abnormal formations. Therefore, this new model can serve a dual purpose in the study of PDAC.

Future work with this model should include more aspects of the cellular microenvironment to make it more physiologically relevant. There are many cell types that are present in the surrounding *in vivo* microenvironment such as stromal fibroblasts or immune cells. These cells could be added to the collagen matrix to study the combined effect. Additionally, the ECM of the chip could be altered to include additional elements of the ECM, such as a thin layer of type IV collagen to mimic the basement membrane.

The cell line used here, Panc1-Tet-PTF1a, confirms that inducing only the PTF1a gene is able to turn malignant pancreatic cancer cells into secretory acinar cells. This provides a

promising target for gene therapy methods to treat PDAC. Further work using this chip would explore methods of altering the genome of cells as they are being cultured within the chip to restore the function of the PTF1a gene. This *in vitro* platform it would provide a quick and simple preliminary test of gene therapy methods before experiments involving animal models.

While the geometry of the chip closely mimics *in vivo* acini, this platform yields an acinus many times larger than those found naturally. Due to fabrication constraints in the present work, this disparity in scale was deemed acceptable, but future work could be done to more accurately represent the size of a pancreatic acinus if needed. The current work with this model showed very successful results in mimicking the acinar microenvironment *in vitro*, and many adaptations can be made to further improve the platform, making this model a very promising option for pancreatic research.

## REFERENCES

- [1] American Cancer Society, “Survival rates for exocrine pancreatic cancer,” 2016. [Online]. Available: <https://www.cancer.org/cancer/pancreatic-cancer/detection-diagnosis-staging/survival-rates.html#references>.
- [2] R. H. Hruban, R. E. Wilentz, and S. E. Kern, “Genetic progression in the pancreatic ducts,” *Am. J. Pathol.*, vol. 156, no. 6, pp. 1821–1825, 2000.
- [3] A. L. Cubilla and P. J. Fitzgerald, “Morphological Lesions Associated with Human Primary Invasive Nonendocrine Pancreas Cancer,” *Cancer Res.*, vol. 36, no. July, pp. 2690–2698, 1976.
- [4] T. Welsch, J. Kleeff, and H. Friess, “Molecular Pathogenesis of Pancreatic Cancer: Advances and Challenges,” *Curr. Mol. Med.*, vol. 7, no. 5, pp. 504–521, 2007.
- [5] L. Zhu, G. Shi, C. M. Schmidt, R. H. Hruban, and S. F. Konieczny, “Acinar cells contribute to the molecular heterogeneity of pancreatic intraepithelial neoplasia,” *Am. J. Pathol.*, vol. 171, no. 1, pp. 263–273, 2007.
- [6] N. Habbe *et al.*, “Spontaneous induction of murine pancreatic intraepithelial neoplasia (mPanIN) by acinar cell targeting of oncogenic Kras in adult mice,” *Proc. Natl. Acad. Sci.*, vol. 105, no. 48, pp. 18913–18918, 2008.
- [7] Q. Tu *et al.*, “A novel pancreatic cancer model originated from transformation of acinar cells in adult tree shrew, a primate-like animal,” *Dis. Model. Mech.*, vol. 12, no. 4, p. dmm038703, 2019.
- [8] R. M. M. Ferreira *et al.*, “Duct- and Acinar-Derived Pancreatic Ductal Adenocarcinomas Show Distinct Tumor Progression and Marker Expression,” *Cell Rep.*, vol. 21, no. 4, pp. 966–978, 2017.
- [9] J. M. Bailey *et al.*, “P53 mutations cooperate with oncogenic Kras to promote adenocarcinoma from pancreatic ductal cells,” *Oncogene*, vol. 35, no. 32, pp. 4282–4288, 2016.
- [10] G. Von Figura *et al.*, “The chromatin regulator Brg1 suppresses formation of intraductal papillary mucinous neoplasm and pancreatic ductal adenocarcinoma,” *Nat. Cell Biol.*, vol. 16, no. 3, pp. 255–267, 2014.
- [11] J. P. Morris, S. C. Wang, and M. Hebrok, “KRAS, Hedgehog, Wnt and the twisted developmental biology of pancreatic ductal adenocarcinoma,” *Nat. Rev. Cancer*, vol. 10, no. 10, pp. 683–695, 2010.
- [12] I. Rooman and F. X. Real, “Pancreatic ductal adenocarcinoma and acinar cells: A matter of differentiation and development?,” *Gut*, vol. 61, no. 3, pp. 449–458, 2012.

- [13] P. Storz, "Acinar cell plasticity and development of pancreatic ductal adenocarcinoma," vol. 14, no. 5, pp. 296–304, 2017.
- [14] J. L. Kopp *et al.*, "Identification of Sox9-Dependent Acinar-to-Ductal Reprogramming as the Principal Mechanism for Initiation of Pancreatic Ductal Adenocarcinoma," *Cancer Cell*, vol. 22, no. 6, pp. 737–750, 2012.
- [15] G. Shi, D. Drenth, C. Qu, D. Barney, D. Miley, and S. F. Konieczny, "Maintenance of acinar cell organization is critical to preventing Kras-induced acinar-ductal metaplasia," *Oncogene*, vol. 32, no. 15, pp. 1950–1958, 2013.
- [16] X. Liu *et al.*, "Genetic ablation of smoothensin in pancreatic fibroblasts increases acinar-ductal metaplasia," *Genes Dev.*, vol. 30, no. 17, pp. 1943–1955, 2016.
- [17] A. Hoorens *et al.*, "Pancreatic acinar cell carcinoma. An analysis of cell lineage markers, p53 expression, and Ki-ras mutation," *Am. J. Pathol.*, vol. 143, no. 3, pp. 685–98, 1993.
- [18] O. A. Mareninova, A. I. Orabi, and S. Z. Husain, "Experimental acute pancreatitis : In vitro models 2 . Acinar Cell Preparations," pp. 1–16, 2015.
- [19] L. Singh, D. K. Bakshi, R. K. Vasishta, S. K. Arora, S. Majumdar, and J. D. Wig, "Primary culture of pancreatic (human) acinar cells," *Dig. Dis. Sci.*, vol. 53, no. 9, pp. 2569–2575, 2008.
- [20] X. Zhao, J. Han, and C. Tang, "Primary culture of porcine pancreatic acinar cells," *Pancreas*, vol. 2, no. 2, pp. 78–82, 2002.
- [21] K. H. Song *et al.*, "In vitro transdifferentiation of adult pancreatic acinar cells into insulin-expressing cells," *Biochem. Biophys. Res. Commun.*, vol. 316, no. 4, pp. 1094–1100, 2004.
- [22] R. Tamizhselvi, P. K. Moore, and M. Bhatia, "Hydrogen sulfide acts as a mediator of inflammation in acute pancreatitis: In vitro studies using isolated mouse pancreatic acinar cells," *J. Cell. Mol. Med.*, vol. 11, no. 2, pp. 315–326, 2007.
- [23] N. M. Krah *et al.*, "The acinar differentiation determinant PTF1A inhibits initiation of pancreatic ductal adenocarcinoma," *Elife*, vol. 4, no. JULY2015, pp. 1–25, 2015.
- [24] B. L. Jakubison *et al.*, "Induced PTF1a expression in pancreatic ductal adenocarcinoma cells activates acinar gene networks, reduces tumorigenic properties, and sensitizes cells to gemcitabine treatment," *Mol. Oncol.*, vol. 12, no. 7, pp. 1104–1124, 2018.
- [25] K. E. Sung and D. J. Beebe, "Microfluidic 3D models of cancer," *Adv. Drug Deliv. Rev.*, vol. 79, pp. 68–78, 2014.
- [26] A. Abbott, "Biology's new dimension," vol. 424, pp. 870–872, 2003.

- [27] K. Chwalek, L. J. Bray, and C. Werner, "Tissue-engineered 3D tumor angiogenesis models: Potential technologies for anti-cancer drug discovery," *Adv. Drug Deliv. Rev.*, vol. 79, pp. 30–39, 2014.
- [28] S. Lunardi, R. J. Muschel, and T. B. Brunner, "The stromal compartments in pancreatic cancer: Are there any therapeutic targets?," *Cancer Lett.*, vol. 343, no. 2, pp. 147–155, 2014.
- [29] S. Breslin and L. O'Driscoll, "Three-dimensional cell culture: The missing link in drug discovery," *Drug Discov. Today*, vol. 18, no. 5–6, pp. 240–249, 2013.
- [30] Y. Li and K. A. Kilian, "Bridging the Gap: From 2D Cell Culture to 3D Microengineered Extracellular Matrices," *Adv. Healthc. Mater.*, vol. 4, no. 18, pp. 2780–2796, 2015.
- [31] Z. Koledova, *3D cell culture: Methods and Protocols*, vol. 1612. 2017.
- [32] B. Han, C. Qu, K. Park, S. F. Konieczny, and M. Korc, "Recapitulation of complex transport and action of drugs at the tumor microenvironment using tumor-microenvironment-on-chip," *Cancer Lett.*, vol. 380, no. 1, pp. 319–329, 2016.
- [33] A. Chronopoulos, T. J. Lieberthal, and A. E. del Río Hernández, "Pancreatic cancer: a mechanobiology approach," *Converg. Sci. Phys. Oncol.*, vol. 3, no. 1, p. 013001, 2017.
- [34] T. J. Puls, X. Tan, C. F. Whittington, and S. L. Voytik-Harbin, "3D collagen fibrillar microstructure guides pancreatic cancer cell phenotype and serves as a critical design parameter for phenotypic models of EMT," *PLoS One*, vol. 12, no. 11, pp. 1–25, 2017.
- [35] P. Dauer *et al.*, "Inactivation of cancer-associated-fibroblasts disrupts oncogenic signaling in pancreatic cancer cells and promotes its regression," *Cancer Res.*, vol. 78, no. 5, pp. 1321–1333, 2018.
- [36] A. Labernadie *et al.*, "A mechanically active heterotypic E-cadherin/N-cadherin adhesion enables fibroblasts to drive cancer cell invasion," *Nat. Cell Biol.*, vol. 19, no. 3, pp. 224–237, 2017.
- [37] E. W. K. Young, "Cells, tissues, and organs on chips: Challenges and opportunities for the cancer tumor microenvironment," *Integr. Biol. (United Kingdom)*, vol. 5, no. 9, pp. 1096–1109, 2013.
- [38] C. R. Drifka *et al.*, "Periductal stromal collagen topology of pancreatic ductal adenocarcinoma differs from that of normal and chronic pancreatitis," *Mod. Pathol.*, vol. 28, no. 11, pp. 1470–1480, 2015.
- [39] L. L. Bischel, S. H. Lee, and D. J. Beebe, "A Practical method for patterning lumens through ECM hydrogels via viscous finger patterning," *J. Lab. Autom.*, vol. 17, no. 2, pp. 96–103, 2012.



- [40] G. Cox and E. Kable, “Second-Harmonic Imaging of Collagen,” vol. 319, no. 1, pp. 15–35, 2007.
- [41] J. A. Williams, “Regulation of Normal and Adaptive Pancreatic Growth 2 . Measurement of Pancreatic Size 3 . Prenatal Pancreatic Growth,” no. 141, 2017.
- [42] T. Saito and J. Sadoshima, “Abnormalities of the Pancreas in type 1 Diabetes,” vol. 116, no. 8, pp. 1477–1490, 2016.
- [43] E. Afghani, “Introduction to Pancreatic Disease: Chronic Pancreatitis,” *Am. Pancreat. Assoc.*, pp. 1–9, 2015.
- [44] M. V Apte, R. C. Pirola, and J. S. Wilson, “Alcohol and the Pancreas 2 . Epidemiology of alcoholic pancreatitis 3 . Natural History and Clinical Features,” 2016.

## APPENDIX

Molds, shown in Figure A-1, were designed and 3D printed to create the tops and bottoms of each chip. The assembly process is outlined in Figure A-3.

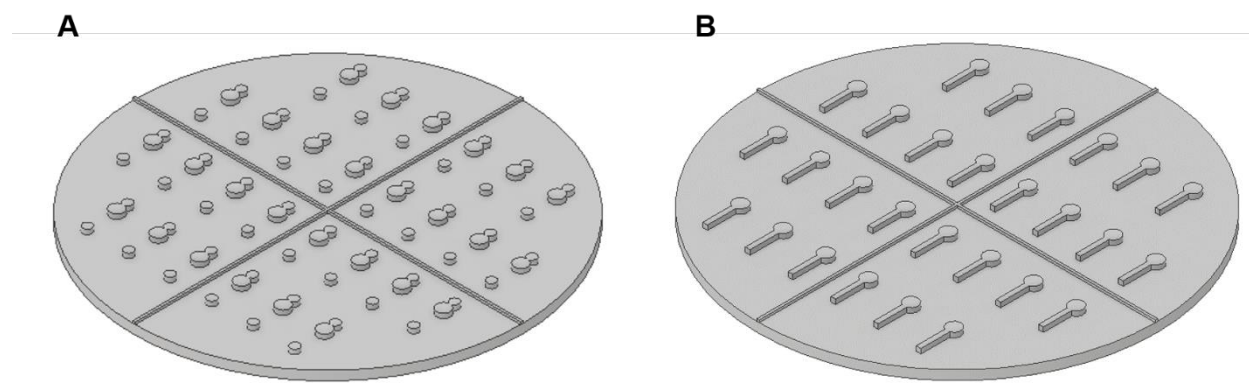


Figure A-1: Molds for the (A) top and (B) bottom of the chip

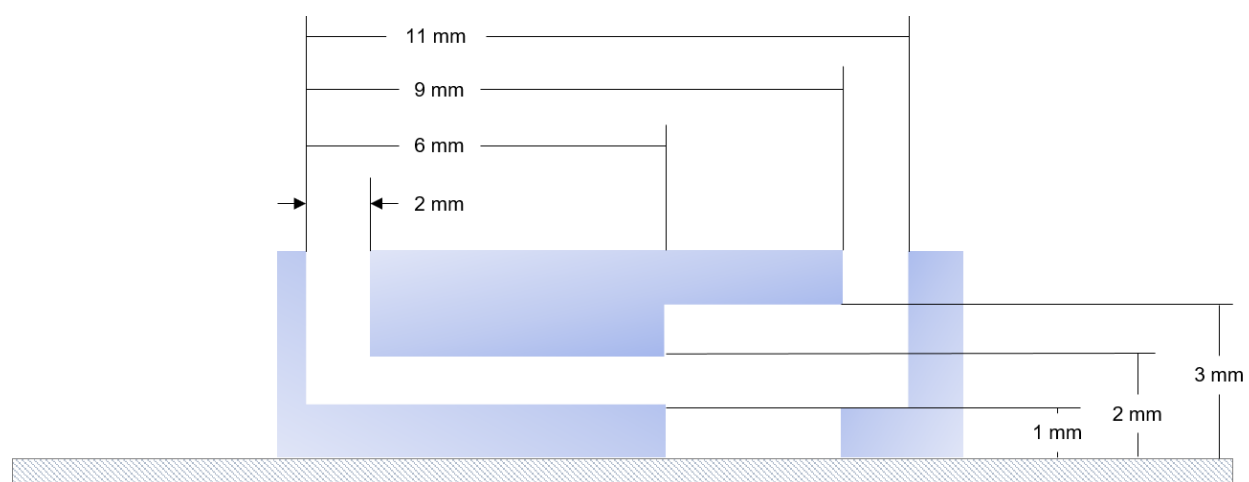


Figure A-2: Side view of assembled chip showing relevant dimensions.

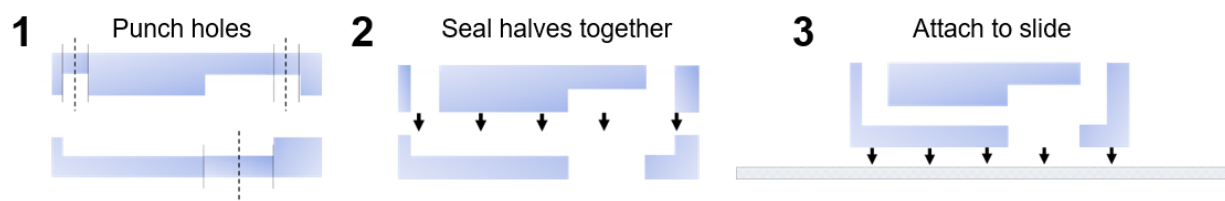


Figure A-3: Chip assembly process

Culture of Panc1 within the AMOC is shown in Figure A-4. This control was performed to confirm that Dox treatment alone was not causing the morphological changes, but rather the expression of PTF1a in the inducible cell line Panc1-Tet-PTF1a. Additionally, it can be seen that Panc1-Tet-PTF1a cells without Dox treatment show the same invasion patterns as Panc1 (without any genetic alteration).

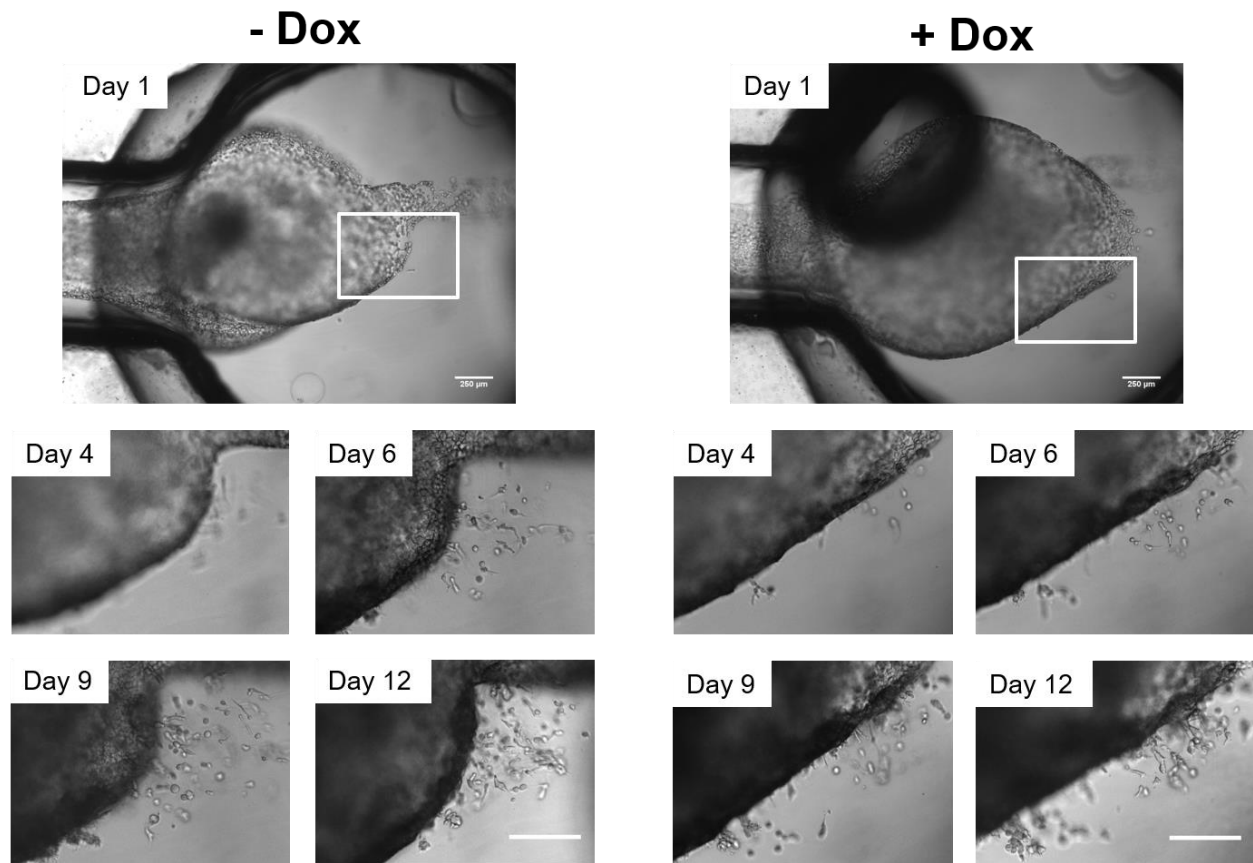


Figure A-4: Panc1 culture with and without Dox. White box in day 1 images show the enlarged region in subsequent days. Scale bars represent 250 μm.

It is possible to treat the cells with doxycycline at two different time points in the experiment: in 2D prior to loading into the chip and in 3D immediately after loading into the chip. Figure A-5 shows that in both cases transcripts for PTF1a and PRSS2 are present. Figure A-6 shows the morphological differences in the first 5 days of culture. Though the growth rate is slower in the 2D induction case yielding fewer cells within the chip, invasion patterns are very similar in that neither case shows any invasion into the matrix. It was decided that the 3D induction method would be used for this study to keep the population of cells loaded into all chips in an experiment constant.

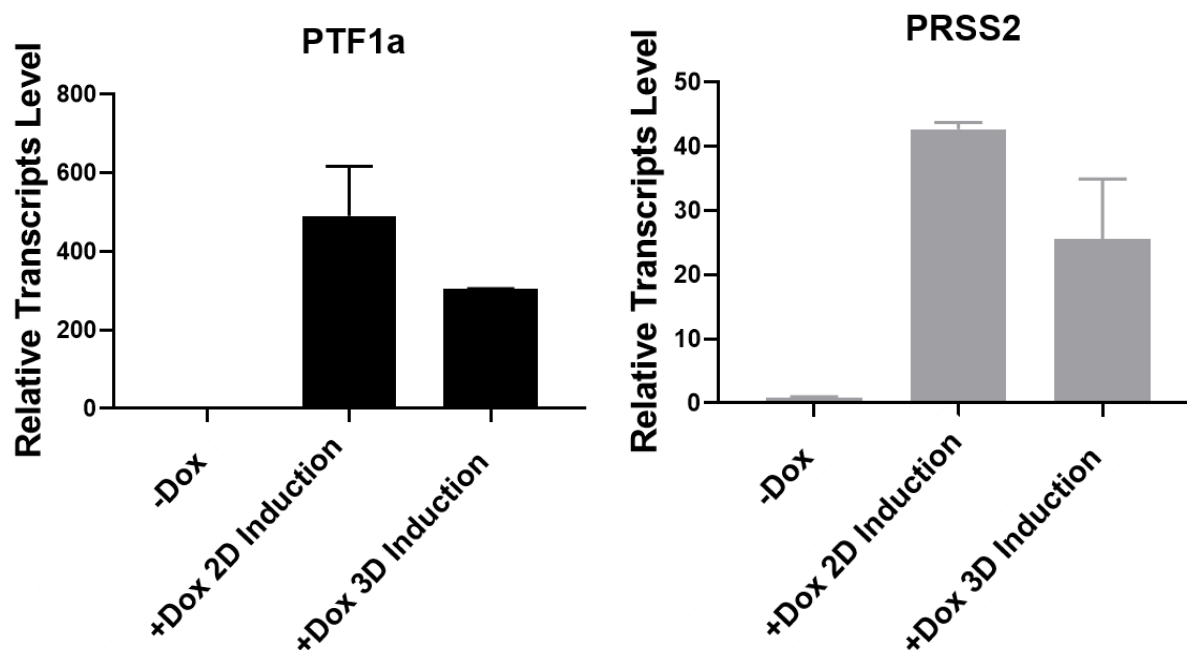


Figure A-5: RT-qPCR results. Relative transcript levels of (A) PTF1a and (B) PRSS2 for 3D culture of the untreated case (-Dox), the case in which the cells first received Dox in 2D (+Dox 2D induction) and the case in which the cells first received Dox treatment once in the chip (+Dox 3D induction)

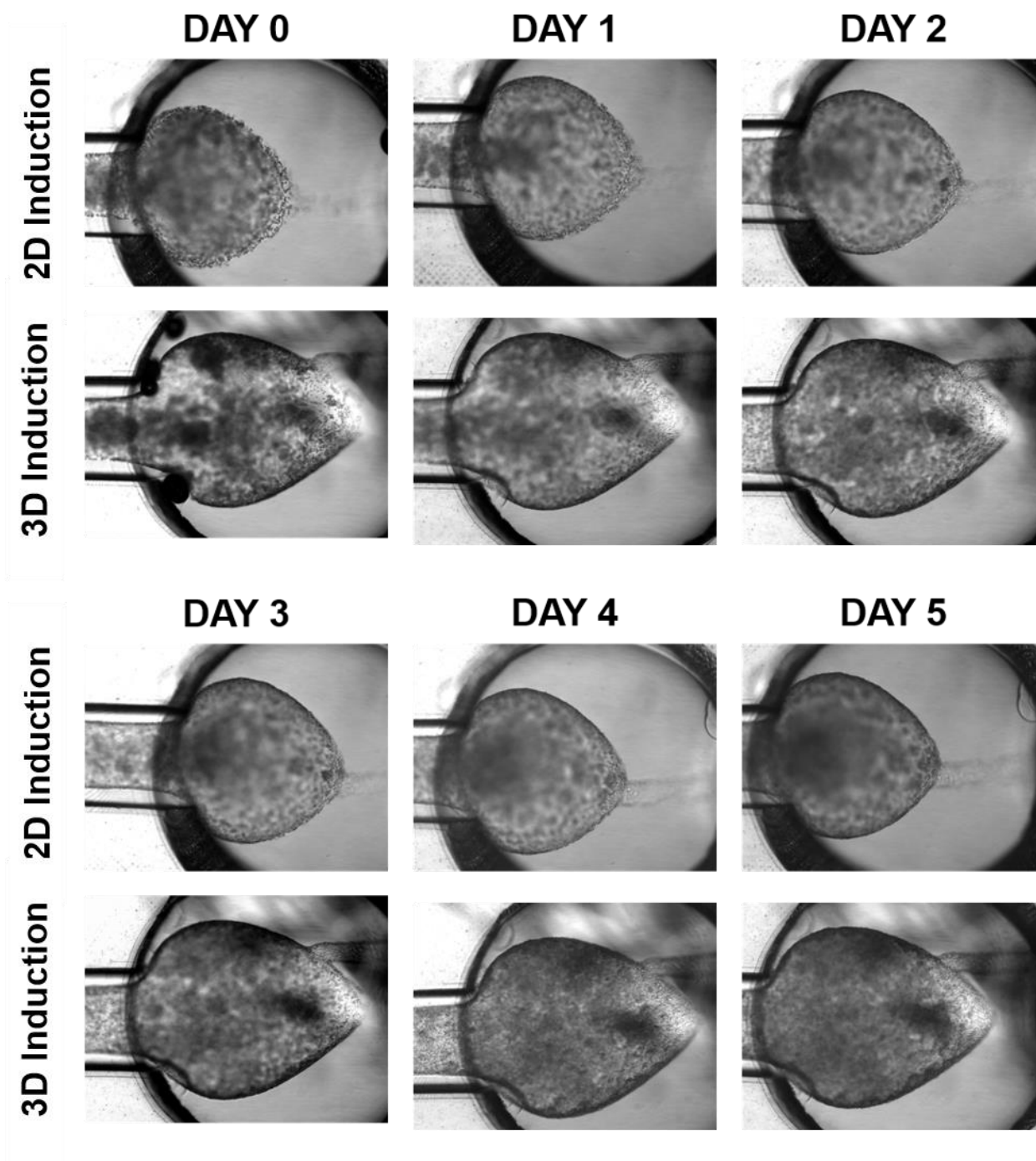


Figure A-6: Morphological comparison of the cells induced 2D and 3D then grown in 3D culture for the first 5 days of culture.